Ionics (2020) 26:3041–3050
https://doi.org/10.1007/s11581-020-03562-0

ORIGINAL PAPER

Electropolymerization of p-phenylenediamine films on carbon fiber fabrics electrode for flexible supercapacitors: surface and electrochemical characterizations

L. M. Samyn[1] · R. Suresh Babu[1] · M. Devendiran[2] · A. L. F. de Barros[1]

Received: 9 October 2019 / Revised: 31 March 2020 / Accepted: 4 April 2020 / Published online: 21 April 2020

Abstract

Supercapacitors are considered as one of the most efficient and reliable approaches to fulfill the specifications of the energy storage devices, owing to high-efficiency storage of energy, which makes supercapacitive electrode materials provoke large curiosity. In this work, we report the electropolymerization of poly(*p*-phenylenediamine) (PpPD) films on lightweight and inexpensive flexible carbon fiber fabrics by potentiostatic technique. The ladder structure of the electrochemically prepared PpPD was examined by Fourier transform infrared spectroscopy (FTIR). The surface characteristics and elemental composition studies were performed through field-emission scanning electron microscope (FESEM) and energy-dispersive X-ray spectroscopy (EDS), which confirmed the polymerization on the carbon fabrics. The electrochemical behavior of the fabricated supercapacitors was investigated by electrochemical analysis including cyclic voltammetry, galvanostatic charge–discharge, and electrochemical impedance spectroscopy. The electrodes presented a good capacitive retention in a sweep rate range between 5 and 100 mV s^{-1} using cyclic voltammetry. The coated electrode exhibited good electrochemical property with a high specific capacitance of 80 F g^{-1} at the current density of 1 A g^{-1}. The high electrochemical performance is associated to the outstanding conductivity, high electrochemical stability, and superior flexibility of the carbon fiber fabrics. The accomplishment of such superior performance, lightweight, and mechanically flexible supercapacitor can stimulate the use in energy storage applications and wearable electronics.

Keywords Supercapacitors · *p*-phenylenediamine · Carbon fiber fabrics · Energy storage · Electropolymerization

Introduction

The search for new materials finds support in several electrochemical applications ranging from biosensors to energy storage devices. Numerous materials have exceptional properties such as strength, flexibility, energy storage capacity, low cost, miniature, and friendly environmental impact which are desirable characteristics for a material to be regarded as promising and economically/environmentally sustainable for these applications. In terms of energy generation, accelerated technological development and increase in energy consumption has led to an unsustainable demand for the energy matrix. This permanent energy crisis and the aggravation of the environmental problems generated by the use of fossil fuels and other sources have led to the search for energy sources and more efficient and ecologically sustainable storage devices, representing a desirable alternative in these times of crisis [1–3].

In recent years, increasing demand for compact and wearable devices has led to the evolution of smaller, flexible, lightweight, and excellent performance in energy storage devices. Advances in nanotechnology have allowed the production of multifunctional materials that can be used in smart textiles

Electronic supplementary material The online version of this article (https://doi.org/10.1007/s11581-020-03562-0) contains supplementary material, which is available to authorized users.

✉ R. Suresh Babu
suresh.rajendran@aluno.cefet-rj.br

L. M. Samyn
leandro.samyn@cefet-rj.br

[1] Laboratory of Experimental and Applied Physics (LaFEA), Centro Federal de Educação Tecnológica Celso Suckow da Fonseca (CEFET/RJ), Av. Maracanã 229, Rio de Janeiro 20271-110, Brazil

[2] Department of Analytical Chemistry, School of Chemical Sciences, University of Madras, Guindy Campus, Chennai, Tamil Nadu 600025, India

combining several properties in one fabric. Conductive textiles carbon fabrics and carbon nanotube fibers come to present promising applications in areas such as wearable electronic devices, biosensors, flexible energy storage, and power generation devices [4–14]. Among the various energy storage applications, supercapacitors (also known as electrochemical capacitors) are one of the most promising energy storage devices owing to their good power density, high energy density, and remarkable stability. It has been exhaustively studied as excellent power sources for the next generation developed in miniaturized all-in-one wearable and consumer electronics. Generally, supercapacitors can be classified in two categories based on different mechanisms of energy storage [12]: (i) electrical double-layer capacitors (EDLCs) and (ii) pseudocapacitors. EDLCs are depending on electrostatic charge accumulation by absorption/desorption of oppositely charged ions formed at the electrolyte/electrode interface; however, pseudocapacitors are depending on rapid and reversible Faradaic reactions on the electrode surface to store energy. Carbon fabrics has been known as lightweight and flexible electrode materials for supercapacitors, constructed by carbon fibers through numerous functional materials such as carbon, polymers, metal oxides, metal hexacyanoferrates, and its composites [4, 13].

So far, the use of polyaniline (PANI) materials for supercapacitors has been very attractive. Owing to its beneficial properties like less expensive, excellent conductivity, facile synthesis added to multiple redox states and well-behaved electrochemistry, supercapacitors may allow high pseudocapacitance [1, 4, 13, 15, 16]. The easy oxidative polymerization of aromatic amines, as aniline, using electrochemical process has been exhaustively studied. However, mechanical degradation of the PANI-based electrode is a real issue. During charging-discharging process, physical degradation caused by swelling and shrinkage may occur, reducing life time and decreasing electrochemical performance. In addition, according to the degradation of PANI, the overoxidation may occur at high potentials, leading to relatively low working potentials of PANI electrodes [17, 18].

Electropolymerization of aromatic diamines (AD) may be more attractive since they exhibit advantages including a novel multifunctionality, heterogeneity of macromolecular structure, and electroconductivity than PANI owing to one amino group is free per repeat unit on the polymers and potentially wide applicability [19, 20]. The application of ortho-, meta-, and para-phenylenediamine-based supercapacitors has been reported earlier. Poly ortho-phenylenediamine (PoPD) was electrochemically polymerized in the presence of sodium dodecyl sulfate (SDS) in indium tin oxide electrode; the resultant electrode achieved the specific capacitance of 106 F g^{-1} at the scan rate of 5 mV s^{-1} in 1 M KNO_3 [21]. Paraphenylenediamine (pPD) is one of the important isomers of phenylenediamine (PD) that belongs to aniline derivatives but shows different properties when compared to it [22]. Graphene/pPD nanocomposites as electrode material for supercapacitor have specific capacitance of 248 F g^{-1} in acidic medium [23]. Chen et al. employed pPD to activate graphene which was meanwhile covered by pPD and the material achieved the specific capacitance of 122 F g^{-1} [24]. Graphene covalently functionalized with PpPD as electrode material for supercapacitors and it exhibits high specific capacitance of 347 F g^{-1} at 1 A g^{-1} [25]. Archana et al. have synthesized and characterized the pPD with and without anionic surfactant in mild acidic conditions and evaluated the changes at the morphology and physical properties [26]. They concluded that the prepared polymer had semiconducting properties which can make this material useful for supercapacitor studies. So far, the use of pPD in supercapacitors was already discussed in [27, 28]. Wu et al. developed a redox medium using pPD and KOH to be used as electrolyte for supercapacitors [27]. The inherent reduction/oxidation states and rapid reversibility properties for Faradaic reactions of the pPD made it appropriate to be used in supercapacitors. It exhibited an increase in the specific capacitances and the energy density when compared using only KOH as electrolyte. Further, more recently, polyaniline nanofibers were prepared with binary oxidant containing ammonium persulfate and ferric chloride at the presence of pPD acting as initiator accelerating the reaction rate [18].

Herein, we demonstrated the application of lightweight carbon fiber fabrics as the base electrode for electropolymerization of pPD-based binder-free and flexible supercapacitor. The one-step deposition of the polymer films on surface of the carbon fiber fabrics (CFFs) electrode having an acid aqueous medium as electrolyte was performed using cyclic voltammetry technique. The selection of the aqueous medium was made since it was already reported in non-aqueous solvents that pPD does not electropolymerize [20]. Despite the studies made so far, the effects of polymerization of pPD in the preparation of carbon fiber electrodes to be used in supercapacitor studies are not clear. The purpose of this article is to investigate the electrodeposition of pPD on carbon fiber in different concentrations using aqueous sulfuric acid solution as medium without the presence of surfactants using cyclic voltammetry technique. The obtained polymer film was characterized and confirmed by FTIR, FESEM, by cyclic voltammetry (CV), and electrochemical impedance spectroscopy (EIS).

Experimental

Chemicals

p-Phenylenediamine was supplied by Sigma Aldrich®. The other chemicals with AnalaR-grade were purchased and used

without any specific treatment. Low-resistance carbon fiber fabrics types RC200P (< 10 Ω) were purchased from Barracuda™, Brazil. Further, double-distilled water was used for all experiments.

Material characterization

The fabricated PpPD/CF electrodes were characterized by FTIR (Agilent Cary 630® FTIR spectrometer, USA) in the range from 4000 to 400 cm^{-1} allowing to see the deposition at the surface of the carbon fiber electrode. The electrode surface morphology was analyzed by FESEM obtained with Thermo Scientific™ Quattro (ThermoFisher Scientific, USA).

The electrochemical behaviors of the fabricated electrodes were analyzed by CV, galvanostatic charge–discharge (GCD), and EIS techniques using the multi-potentiostat (IVIUM Technologies). At room temperature, the three-electrode cell configuration with 1.0 M H_2SO_4 aqueous solution as the electrolyte was used to measure the electrochemical property. The PpPD/CF, platinum sheet, and Ag/AgCl electrodes were used as the working electrodes, counter electrode, and reference electrode, respectively. CVs were performed at various scan rates between 5 and 100 mV s^{-1}. The EIS was evaluated under the half-wave potential (E^0) by sweeping the frequency between 1 Hz and 100 kHz at amplitude of 50 mV.

From the experiment results, the values of specific capacitance were calculated by integrating the CV profile of the working electrode (current versus potential) by means of the following equation [29–32]:

$$S_{pC} = \frac{1}{2m\vartheta\Delta V}\oint_{V_1}^{V_2} I(V)dV \quad (1)$$

where S_{pC} is the working electrode gravimetric capacitance (F g^{-1}), m is the electroactive material weight coated on the working electrode (g), ϑ is the applied scan rate (V s^{-1}), ΔV is the potential window scanned, and I is the instantaneous current (A) appropriate to CV curves. This equation takes into consideration that the anodic voltammetric charges and cathodic voltammetric charges may not be the same in that the shape of CV curves may not have the ideal mirror symmetry.

From the CV curves, it is possible to observe that there are two different kinds of capacitive contributions: one double-layer capacitance from the carbon fiber and other pseudocapacitance from PpPD redox reactions.

From Eq. (2), the galvanostatic capacitances were calculated using the integral current area of the discharge curve. The quasi-reversible faradaic reactions make the charge/discharge curves non-symmetric turning the integral of the discharge area necessary to determine the energy density [33, 34]:

$$C = \frac{2i\int Vdt}{V^2\big|_{V_1}^{V_2}} \quad (2)$$

where S_{pC} is the gravimetric capacitance of the working electrode (F g^{-1}), m is the weight of the electroactive material of the electrode (g), $\int Vdt$ is the integral current area of the discharge curve, where V is the potential window with the initial and final value of V_1 and V_2, respectively.

Electrode fabrication

The CFF were cut at the desired size (1.0 cm × 1.0 cm) and a few stitches were done for better fixation of the material. No additional preparation was done since CFF material was mechanically strong and flexible and has high conductivity and very low weight. The p-phenylenediamine was deposited into CFF electrodes by electropolymerization method using cyclic voltammetry with four different concentrations (1, 3, 5, and 10 mM) with 50 mL each one containing 1.0 M of H_2SO_4 as electrolyte. After drying in ambient temperature, the electrodes were cleaned with distilled water several times to eliminate the monomers and unbound polymer materials on the surface of electrode and dried in room temperature overnight. The mass of the coated active material on the CFF electrode surface was optimized at approximately 1.0 mg cm^{-2}. Figure 1a demonstrates the polymerization setup and Fig. 1b the snapshot of the bare carbon fiber electrode.

Results and discussion

Mechanism of PpPD electrochemical polymerization

The electrochemical polymerization of pPD on the surface of carbon fiber fabrics electrode was made by cyclic voltammetry (CV) technique in the potential window between − 0.2 and 1.2 V during 50 continuous cycles at a sweep rate of 50 mV s^{-1} in 1 M H_2SO_4 (see supplementary information Fig. S1). Figure 2a shows all polymerization cycles for

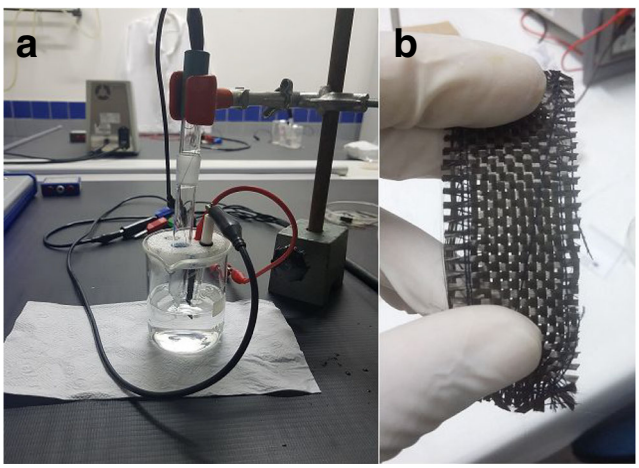

Fig. 1 Electrodeposition apparatus **a** three electrodes cell experimental setup and **b** flexible carbon fiber fabrics

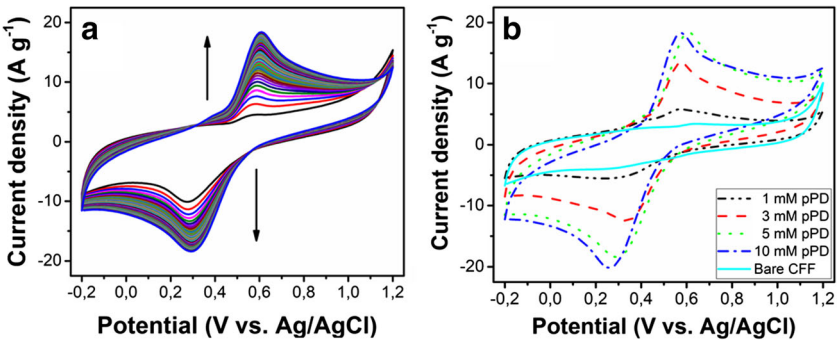

Fig. 2 CV curves of pPD electropolymerization **a** 50 continuous cycles for 5 mM pPD concentration and **b** 50th cycle of 1, 3, 5, and 10 mM pPD for comparison

5 mM pPD in the electrode surface at a sweep rate of 50 mV s^{-1}. From the peaks, it is possible to see the reversibility of the process and that the repetitive cycling leads to the formation of the polymer film. With the increase of the concentration, it is possible to see the current density growth. Figure 2b shows a comparison between the last cycles of polymerization of all electrodes and a bare carbon fiber electrode. At concentration of 5 mM, the current reaches more than three times the one of 1 mM concentration. In concentration of 10 mM, the current density does not increase much compared with the 5 mM electrode. All the cases of CV display a pair of well-defined redox peaks. The oxidation peak at + 600 mV may be associated with removal of an electron from one of the amino group nitrogen to form the radical cation, which occurs after adsorption of the monomer on the carbon fiber fabrics. Subsequently, the cleavage of C–N bond forms a radical cation that attacks other monomer pPD molecule leading to the formation of semiquinone radical cation (polaron state), and the suggested growing mechanism of the prepared PpPD is illustrated in Scheme 1. On backward scan, the cathodic current increase indicates the presence of PpPD polymer layer adhered to the CFF electrode surface. Near from + 300 mV, one cathodic peak was formed and might be ascribed to the reduction reaction of the radical cation to the pPD monomer (conjugated to the anodic peak) [16, 34]. On continuous cycling, the CVs identical to that of the second scan are attained showing progressive growth of the PpPD on the electrode surface with the corresponding increases in the current density with the number of scans.

FTIR spectroscopy

The FTIR spectra for the PpPD/CF electrodes with different molar ratios are presented in Fig. 3 for a convenient comparison and allowing the identification of the functional groups present in the polymer film [16, 25, 34]**.** The infrared vibration bands for the monomer and the PpPD at the carbon fiber shown at the spectra are in accordance with previous reports. The pPD monomer showed peaks around 3372 and 3301 cm^{-1} regarding NH_2 asymmetric stretching vibration of aromatic amine [34]. Those peaks did not appear at the PpPD spectra. The band at 1505 cm^{-1} was attributed to the stretching vibrations of C=N bond of phenazine ring [25]. The peak at 1406 cm^{-1} is the characteristic stretching vibrations of

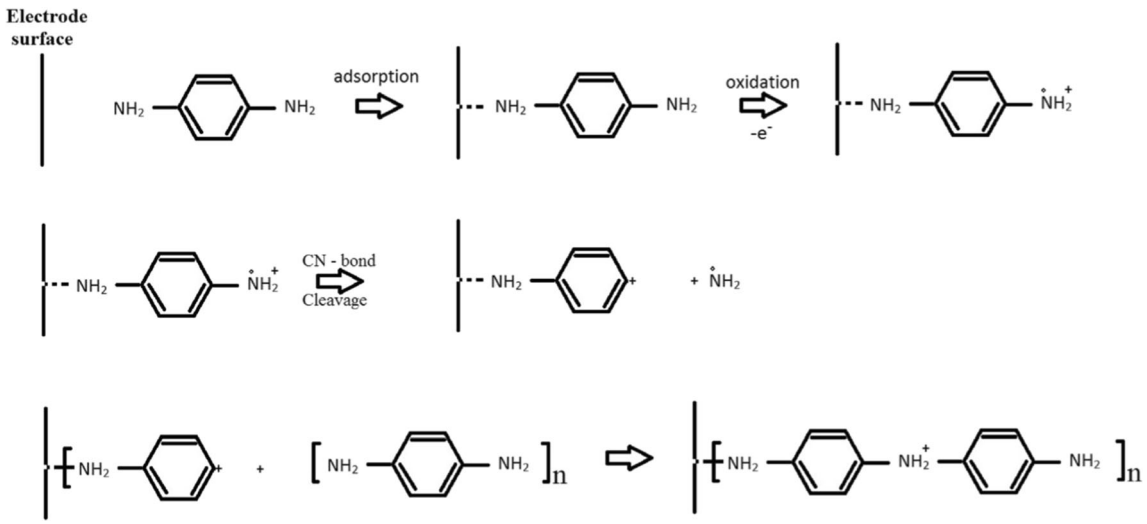

Scheme 1 Suggested growing mechanism of the prepared PpPD

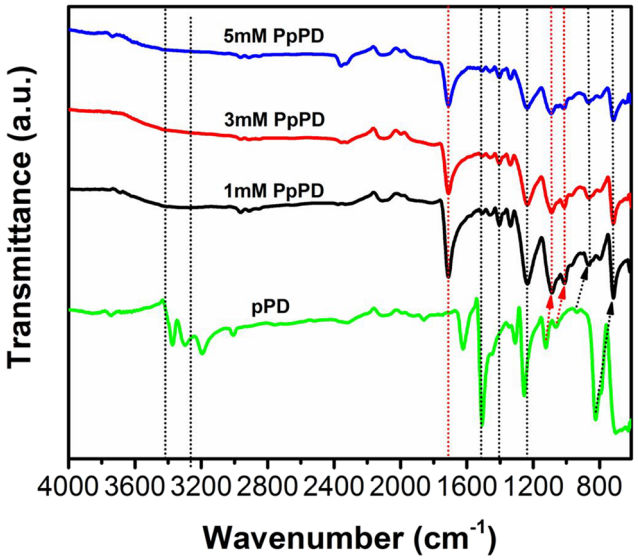

Fig. 3 FTIR spectra of pPD monomer and PpPD-coated electrodes for 1 mM, 3 mM, and 5 mM concentrations

C–N–C linkage of benzenoid and quinoid imine units [25]. The peak at 1236 cm^{-1} is ascribed with the stretching vibration of C–N bond of benzonoid ring [16, 33]. The peaks at 820 and 805 cm^{-1} can be attributed to the out-of-plane bending stretching vibration of the benzene ring [25, 35]. These peaks give indications of the formation of PpPD film in the carbon fiber.

FESEM and EDS mapping

The surface morphology of the different PpPD/CF fabricated electrodes was studied through FESEM analysis. Figure 4a, c, and e shows the low-magnification FESEM of the PpPD/CFF electrode with 1 mM, 3 mM, and 5 mM concentrations. It is possible to see unidirectional carbon fiber with around 5 μm diameter with enough gap to another carbon fiber and enough pores of individual fibers, which helps for more wettability of electrolyte and the polymer coating evenly throughout the electrode surface. Enlarging the image with higher magnification (Fig. 4b–f) is possible to see the homogenous polymerization by PpPD at the surface of the carbon fiber. Figure 4d shows clearly the faceted plate-like particles with a wide size distribution, which confirms that the pPD get polymerized. Figure 4e shows the FESEM of the electrode with the highest pPD concentration (5 mM). With a good approximation of the electrode (Fig. 4f) it is possible to see the good adhesion and homogeneous distribution of the PpPD polymer at the surface of the CFF electrode.

Fig. S2 presents the EDS spectra to confirm the existence of N, O, and S in the surfaces of CFF electrode. The elemental

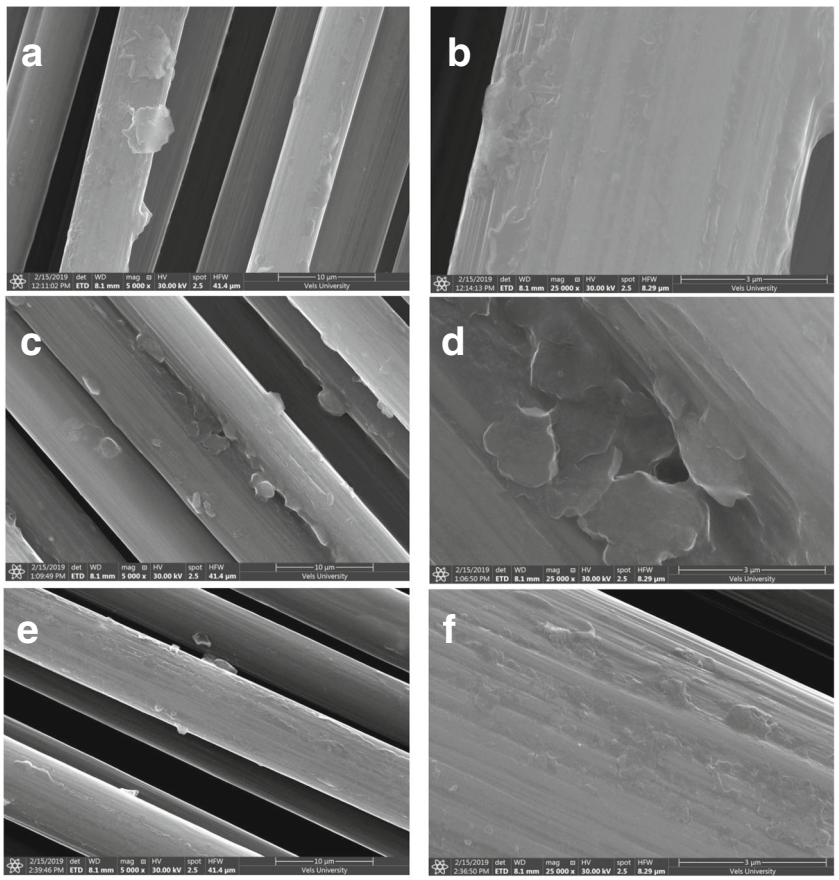

Fig. 4 FESEM images of the coated CFF with **a** 1 mM PpPD, **b** 1 mM single fiber detail, **c** 3 mM PpPD, **d** 3 mM single fiber detail, **e** 5 mM PpPD, and **f** 5 mM single fiber detail

Table 1 Elemental composition for the polymerized electrodes with different PPD concentrations

Material	*C* (wt%)	*N* (wt%)	*O* (wt%)	Al (wt%)	*Si* (wt%)	*S* (wt%)	Ca (wt%)
1 mM	72.26	18.21	8.37	–	0.26	0.90	–
3 mM	61.17	19.86	17.78	0.23	0.65	0.31	–
5 mM	75.55	19.54	4.27	–	–	0.52	0.12
Error	± 0.68	± 4.46	± 1.46	± 0.04	± 0.05	± 0.07	± 0.03

compositions are shown in Table 1. Nevertheless, peaks from the substrate and electrolyte (Si, S, and O) were inevitable since the formed coating is thin. The images of EDS mapping confirmed that carbon is the predominant component in the electrodes with some small peaks of nitrogen from the formed coating. To highlight the coating at the surface of the carbon fibers, elemental maps were taken and presented in supplementary information (Fig. S3, S4 and Fig. S5 for 1, 3, and 5 mM, respectively).

Electrochemical characterization

Effect of scan rate The electrochemical performance of the different concentrations of PpPD electrodes was investigated in 1.0 M H_2SO_4 electrolyte by cyclic voltammetry at different sweep rates ranging from 5 to 100 mV s^{-1} (Fig. 5a–c). It is possible to observe that the oxidation and the reduction peak currents increase with the sweep rate increases. The CV curves exhibit a hybrid behavior with EDLC and pseudocapacitive compounds. The EDLC is inherent to the porosity and conductivity of the carbon fiber fabrics materials. The pseudocapacitive peaks are assigned to the redox properties of the PpPD, and obviously, the current density was increased when the pPD concentration increases. As described previously, the oxidation and reduction peaks typical from the polymerization of pPD at the electrode surface are clearly exhibited during scan rate performances. The obtained voltammogram exhibits an oxidation peak near from + 600 mV (versus Ag/AgCl) and the respective reduction peak can be seen approximately at + 260 mV (versus Ag/AgCl), according to the predicted [12, 26]. From Eq. (1), the specific capacitance values were calculated against the scan rate and can be seen in Fig. 5d. It is possible to observe that the increase in the concentration of pPD takes to a higher specific capacitance value. In all cases, a good stability is noticed even with the increase in the scan rate (~ 20 times).

Galvanostatic charge–discharge The GCD curves of PpPD/CF-fabricated electrodes were examined at various current densities, ranging from 1 to 5 A g^{-1} in the potential range from 0 to 0.6 V as shown in Fig. 6a–c. The measurements confirmed its eligibility for applications as supercapacitors

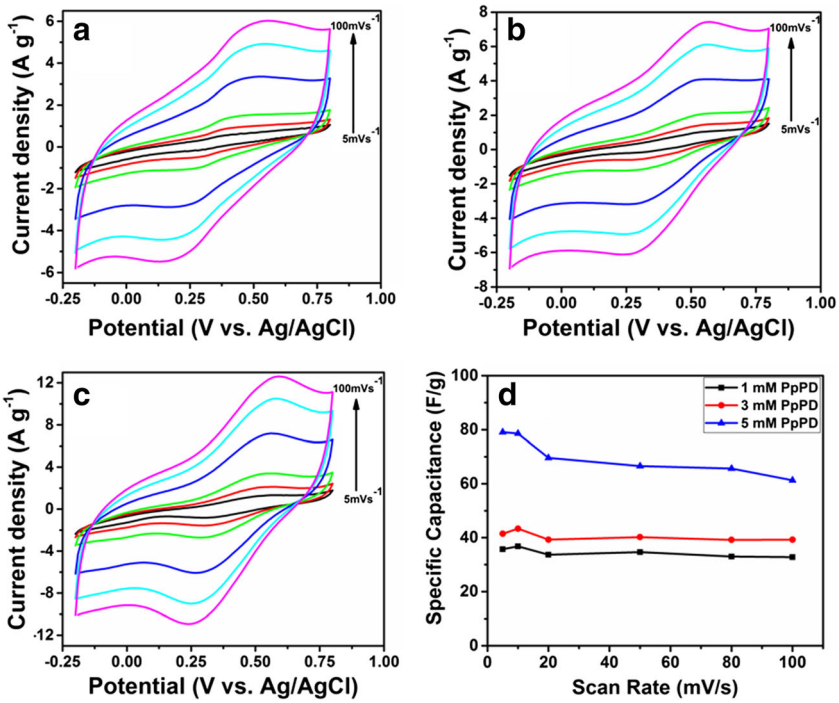

Fig. 5 CV curves of PpPD electrodes at various sweep rates in the potential window between − 0.20 and 0.80 V (vs. Ag/AgCl) **a** 1 mM PpPD, **b** 3 mM PpPD, **c** 5 mM PpPD, and **d** specific capacitance comparison at various sweep rates

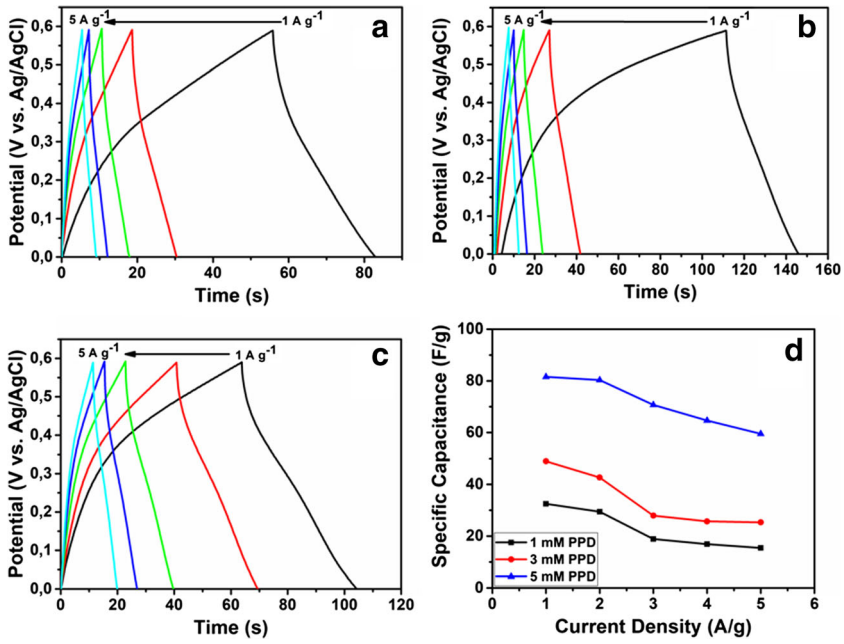

Fig. 6 GCD curves at various current densities of PpPD carbon fiber fabric electrodes within an operating potential window from 0 to 0.60 V (vs. Ag/AgCl) at various current densities from 1 to 5 A g^{-1} **a** 1 mM PpPD, **b** 3 mM PpPD, **c** 5 mM PpPD, and **d** specific capacitance comparison at various current densities

materials. Results show that these coated electrodes present the best behavior with 1 A g^{-1} and small IR drop at the initiation of discharge curve. Generally, this IR drop is associated to the internal resistance and ionic conductivity [25]. The hybrid behavior of the coated electrodes can be identified with regarded to the combination of the two energy-storage process improving its total capacitance. The pseudocapacitance is generated by the reduction/oxidation reactions at the electrode–electrolyte interface and the electrical double layer capacitance on the carbon fiber electrode surface. Using Eq. (2), the gravimetric specific capacitance was determined from the discharge curves of the GCD profiles and the corresponding results are shown in Fig. 6d. The 5 mM PpPD electrode showed the highest specific capacitance of 80 F g^{-1} at a current density of 1 A g^{-1}, which is higher or comparable to the low molecular weight polymer–based supercapacitor electrode materials, such as porous polymeric organic framework of phloroglucinol and terephthaldehyde [36], hypercrosslinked polymer of pyrene and polyaniline [37] and nitrogen-doped carbon nanograss [38].

The capacitance of the carbon fiber without coating is about 6 mF far below from the capacitance obtained for all coated electrodes (Fig. S6). The coulombic efficiency (%) of the supercapacitor can be calculated from the galvanostatic charge–discharge experiments as Eq. (3) and the results are given in Table 2:

$$\eta = \frac{\Delta t_D}{\Delta t_C} \times 100\% \tag{3}$$

where Δt_C and Δt_D are the times of charging and discharging, respectively. According to the results, the average coulombic efficiency is about 64%, 60%, and 72% for 1 mM, 3 mM, and 5 mM PpPD, respectively.

The cyclic stability and reversibility of the as-prepared electrode are important for its application as supercapacitor electrode. The cyclic performance of 5 mM PpPD was further examined by galvanostatic charge–discharge tests for 1000 cycles in the voltage range of 0.0 to 0.6 V with 2 A/g in three-electrode system. From the Fig. 7, it can be seen that there is only 4.4% decay in the available capacity over 1000 cycles. This implies an excellent long-term cycling capability offered by the electrode.

Electrochemical impedance spectroscopy The behavior of hybrid electrode materials applied to supercapacitors involves different storage mechanisms and ion transport phenomena that can be analyzed from EIS data. Using Nyquist plot, obtained from EIS, the frequency response of the assembled system can be fully appreciated giving information about processes occurring in both parts. Generally, Nyquist plots

Table 2 Comparison of the Coulombic efficiency with different concentration of PpPD electrodes

Current (A g^{-1})	Coulombic efficiency (η%)		
	1 mM PpPD	3 mM PpPD	5 mM PpPD
1	49.64	32.52	64.58
2	63.10	60.16	71.92
3	67.30	66.67	74.56
4	69.44	70.33	75.32
5	69.81	71.02	75.22

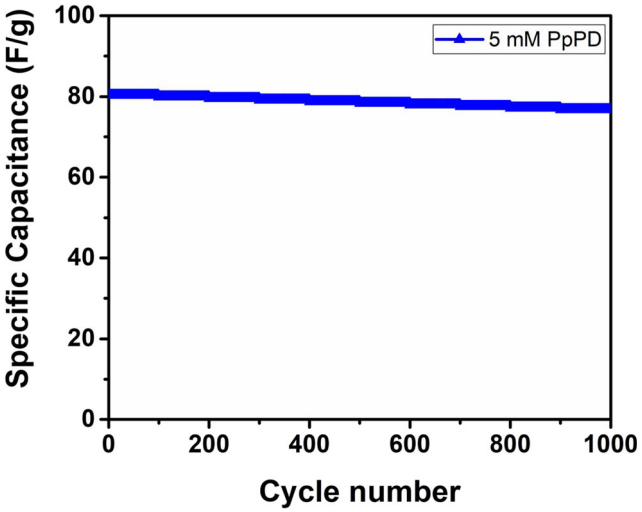

Fig. 7 Coulombic efficiency of the supercapacitor calculated from the galvanostatic charge–discharge experiments

present the complex impedance (real part Z′ versus imaginary part Z). Those results are interpreted by fitting with the experimental results by an equivalent electrical circuit. Figure 8a–c shows the fitted Nyquist plots of 1 mM, 3 mM, and 5 mM PpPD/CF electrodes and Fig. 8d the equivalent circuit obtained from the frequency response. The first point in the diagram shows the intercept of the semicircle with the real part and usually is interpreted as solution resistance of the electrolyte. Herein, the solution resistance (R_s) was associated with both the internal resistance electrode materials and ohmic resistance of the electrolyte, instead of only the electrolyte resistance; otherwise, the resistance would be the same for all three

Table 3 Parameters obtained from the fitted data of corresponding equivalent circuit elements

Electrode	R_s (Ω)	R_{ct} (Ω)	$W \times 10^{-2}$ (Ω)	$C \times 10^{-3}$ (F)	$C_{dl} \times 10^{-6}$ (F)
1 mM	3.47	1.06	3.16	17.00	8.93
3 mM	2.00	0.57	7.83	21.95	29.72
5 mM	2.20	0.59	5.96	22.75	37.83

experiments given that the same electrolyte was utilized. In the high-frequency region, the semicircle is associated to the charge transfer resistance (R_{ct}) combined to the capacitance of the double layer formed by adsorbed ions in the electrode surface (C_{dl}). Its diameter often represents the electrode material resistance combined with the coated material resistance and current collectors resistance. The ion diffusion is clearly observed in the medium frequencies and can be described by Warburg element (W). The equivalent circuit values are summarized in Table 3. It is possible to note that the solution resistance value dropped with the increase of the pPD concentration. The low resistance value for all three electrodes specifies the good conductivity of the carbon fiber. Also, the lowest resistance in 3 mM concentration shows clearly the good properties of the pPD and the good interaction between the coated fibers with the 1.0 M H_2SO_4 electrolyte gives less resistance than the 1 mM electrode. The small increase in the 5 mM electrode may be justified by the mathematical approach in the equivalent circuit calculation. Nevertheless, the non-decrease in resistance may indicate the saturation of the polymerization in higher concentration (compared to

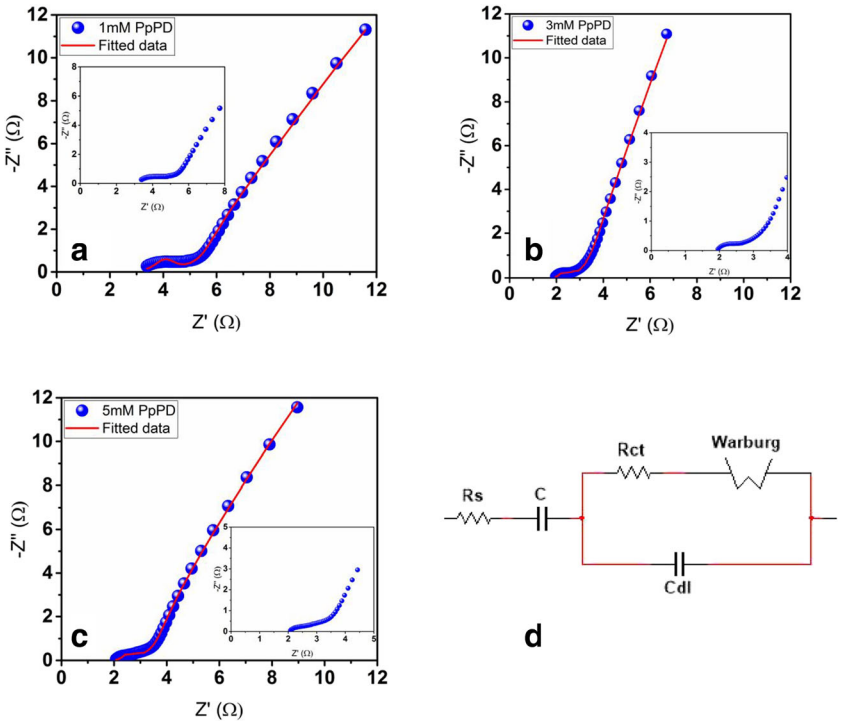

Fig. 8 Nyquist plots of the coated electrodes **a** 1 mM PpPD, **b** 3 mM PpPD, **c** 5 mM PpPD, and **d** equivalent circuit obtained by the frequency response

3 mM) or the increasing of the resistance with the growth of the film. This may justify the current density was not increased during the polymerization process of the 10 mM electrode.

Conclusions

The flexible PpPD films on carbon fiber fabrics were fabricated by facile one-step electropolymerization using cyclic voltammetry method. The as-designed PpPD/CF electrodes were characterized by spectroscopic and microscopic analysis, showing the confirmation of coating in electrode surface. The electrochemical measurements established that the PpPD film can be directly used for supercapacitors, displaying a high specific capacitance of 80 F g^{-1} in 1 M H_2SO_4, as calculated from the CV profile at a sweep rate of 5 mV s^{-1}. The galvanostatic capacitance was also calculated showing a value in good agreement to the capacitance obtained using the CV method. An average coulombic efficiency of 72% for 5 mM PpPD with 2 A/g was achieved. Furthermore, there is only 4.4% decay in the cyclic capability retention over 1000 cycles. Moreover, the steady, robust, and compatible PpPD film is the excellent modification method of fabricating various types of pseudocapacitors to augment the capacitance behaviors. This attempt stimulates a practical elucidation for effortless, low cost, eco-friendly, lightweight, highly flexible, large-scale, and high-performance energy storage devices.

Funding information This research work was supported by the Brazilian agencies such as CNPq (301868/2017-4), CAPES (BEX 5383/15-3), and FAPERJ (E-26/110.087/2014, /213.577/2015 and /216.730/2015). Dr. R. S. Babu received financial support from CAPES in the form of PNPD Fellowship.

References

1. Sharma K, Pareek K, Rohan R, Kumar P (2019) Flexible supercapacitor based on three-dimensional cellulose/graphite/polyaniline composite. Int J Energy Res 43:604–611. https://doi.org/10.1002/er.4277
2. Wen X, Dong T, Liu A, Zheng S, Chen S, Han Y, Zhang S (2018) A new solid-state electrolyte based on polymeric ionic liquid for high-performance supercapacitor. Ionics 25:1–11. https://doi.org/10.1007/s11581-018-2582-7
3. Wang H, Lin J, Shen ZX (2016) Polyaniline (PANi) based electrode materials for energy storage and conversion. J Sci Adv Mat Dev 1:225–255. https://doi.org/10.1016/j.jsamd.2016.08.001
4. Babu RS, de Barros ALF, de Almeida MM, da Motta SD, Balamurugan J, Lee JH (2018) Novel polyaniline/manganese hexacyanoferrate nanoparticles on carbon fiber as binder-free electrode for flexible supercapacitors. Compos Part B: Eng 143:141–147. https://doi.org/10.1016/j.compositesb.2018.02.007
5. Guo J, Zhang Q, Sun J, Li C, Zhao J, Zhou Z, Zhang J (2018) Direct growth of vanadium nitride nanosheets on carbon nanotube fibers as novel negative electrodes for high-energy-density wearable fiber-shaped asymmetric supercapacitors. J Power Sources 382:122–127. https://doi.org/10.1016/j.jpowsour.2018.02.034
6. Li Q, Zhang Q, Sun J, Liu C, Guo J, He B, Yao Y (2019) All hierarchical core–shell heterostructures as novel binder-free electrode materials for ultrahigh-energy-density wearable asymmetric supercapacitors. Adv Sci 6:1801379. https://doi.org/10.1002/advs.201801379
7. Zhou Z, Zhang Q, Sun J, He B, Guo J, Li Q, Yao Y (2018) Metal–organic framework derived spindle-like carbon incorporated α-Fe2O3 grown on carbon nanotube fiber as anodes for high-performance wearable asymmetric supercapacitors. ACS Nano 12:9333–9341. https://doi.org/10.1021/acsnano.8b04336
8. Bavio MA, Acosta GG, Kessler T (2015) Energy storage in symmetric and asymmetric supercapacitors based in carbon cloth/polyaniline-carbon black nanocomposites. Int J Energy Res 39:2053–2061. https://doi.org/10.1002/er.3441
9. Yuksel R, Unalan HE (2015) Textile supercapacitors-based on MnO_2/SWNT/conducting polymer ternary composites. Int J Energy Res 39:2042–2052. https://doi.org/10.1002/er.3439
10. Ng CH, Lim HN, Lim YS, Chee WK, Huang NM (2015) Fabrication of flexible polypyrrole/graphene oxide/manganese oxide supercapacitor. Int J Energy Res 39:344–355. https://doi.org/10.1002/er.3247
11. Kim WJ, Ko TH, Seo MK, Chung YS, Kim HY, Kim BS (2018) Engineered carbon fiber papers as flexible binder-free electrodes for high-performance capacitive energy storage. J Ind Eng Chem 59:277–285. https://doi.org/10.1016/j.jiec.2017.10.033
12. Li L, Lou Z, Chen D, Jiang K, Han W, Shen G (2018) Recent advances in flexible/stretchable supercapacitors for wearable electronics. Small 14:1702829. https://doi.org/10.1002/smll.201702829
13. Maier MA, Babu RS, Sampaio DM, de Barros ALF (2017) Binder-free polyaniline interconnected metal hexacyanoferrates nanocomposites (metal = Ni, Co) on carbon fibers for flexible supercapacitors. J Mater Sci Mater Electron 28:17405–17413. https://doi.org/10.1007/s10854-017-7674-z
14. Pu X, Li L, Liu M, Jiang C, Du C, Zhao Z, Wang ZL (2016) Wearable self-charging power textile based on flexible yarn supercapacitors and fabric nanogenerators. Adv Mater 28:98–105. https://doi.org/10.1002/adma.201504403
15. Eftekhari A, Li L, Yang Y (2017) Polyaniline supercapacitors. J Power Sources 347:86–107. https://doi.org/10.1016/j.jpowsour.2017.02.054
16. Lakard B, Herlem G, Lakard S, Fahys B (2003) Ab initio study of the polymerization mechanism of poly(p-phenylenediamine). J Mol Struc-THEOCHEM 638:177–187. https://doi.org/10.1016/S0166-1280(03)00567-0
17. Zhou SX, Tao XY, Ma J, Qu CH, Zhou Y, Guo LT, Feng PZ, Zhu YB, Wei XY (2017) Facile synthesis of self-assembled polyaniline nanorods doped with sulphuric acid for high-performance supercapacitors. Vacuum 143:63–70. https://doi.org/10.1016/j.vacuum.2017.05.028
18. Qian PF, Li T, Liang BL, Qin ZY (2017) Polyaniline nanofibers prepared with binary oxidant at the presence of para-phenylenediamine. Mater Sci Forum 898:2354–2359. https://doi.org/10.4028/www.scientific.net/MSF.898.2354
19. Pham QL, Haldorai Y, Nguyen VH, Tuma D, Shim JJ (2011) Facile synthesis of poly (p-phenylenediamine)/MWCNT nanocomposites and characterization for investigation of structural effects of carbon nanotubes. Bull Mater Sci 34:37–43. https://doi.org/10.1007/s12034-011-0049-9
20. Li XG, Huang MR, Duan W, Yang YL (2002) Novel multifunctional polymers from aromatic diamines by oxidative

polymerizations. Chem Rev 102:2925–3030. https://doi.org/10.1021/cr010423z
21. Wang M, Zhang H, Wang C, Hu X, Wang G (2013) Direct electrosynthesis of poly-o-phenylenediamine bulk materials for supercapacitor application. Electrochim Acta 91:144–151. https://doi.org/10.1016/j.electacta.2012.12.087
22. Bilal S, Holze R (2011) Spectroelectrochemistry of poly (o-phenylenediamine): polyaniline-like segments in the polymer structure. Electrochim Acta 56:3353–3358. https://doi.org/10.1016/j.electacta.2011.01.005
23. Jaidev RS (2012) Poly(p-phenylenediamine)/graphene nanocomposites for supercapacitor applications. J Mater Chem 22:18775–18783. https://doi.org/10.1039/c2jm33627h
24. Chen Y, Zhang X, Zhang H, Sun X, Zhang D, Ma Y (2012) High-performance supercapacitors based on a graphene-activated carbon composite prepared by chemical activation. RSC Adv 2:7747–7753. https://doi.org/10.1039/C2RA20667F
25. Liu Z, Zhou H, Huang Z, Wang W, Zeng F, Kuang Y (2013) Graphene covalently functionalized with poly(p-phenylenediamine) as high performance electrode material for supercapacitors. J Mater Chem A 1:3454–3462. https://doi.org/10.1039/c3ta01162c
26. Archana S, Jaya Shanthi R (2014) Synthesis and characterization of poly (p-phenylenediamine) in the presence of sodium dodecyl sulfate. Res J Chem Sci 4:60–67 ISSN 2231-606X
27. Wu J, Yu H, Fan L, Luo G, Lin J, Huang M (2012) A simple and high-effective electrolyte mediated with p-phenylenediamine for supercapacitor. J Mater Chem 22:19025–19030. https://doi.org/10.1039/C2JM33856D
28. Yang CH, Wen TC (1994) Electrochemical copolymerization of aniline and para-phenylenediamine on IrO2-coated titanium electrode. J Appl Electrochem 24:166–178. https://doi.org/10.1007/BF00247789
29. Chen W, Fan Z, Gu L, Bao X, Wang C (2010) Enhanced capacitance of manganese oxide via confinement inside carbon nanotubes. Chem Commun 46:3905–3907. https://doi.org/10.1039/C000517G
30. Ortega PF, dos Santos Junior GA, Montoro LA, Silva GG, Blanco C, Santamaría R, Lavall RL (2018) LiFePO4/mesoporous carbon hybrid supercapacitor based on LiTFSI/imidazolium ionic liquid electrolyte. J Phys Chem C 122:1456–1465. https://doi.org/10.1021/acs.jpcc.7b09869
31. Senthilkumar K, Prabakar SJR, Park C, Jeong S, Lah MS, Pyo M (2016) Graphene oxide self-assembled with a cationic fullerene for high performance pseudo-capacitors. J Mater Chem A 4:1663–1670. https://doi.org/10.1039/C5TA09929C
32. Pandit B, Dubal DP, Sankapal BR (2017) Large scale flexible solid state symmetric supercapacitor through inexpensive solution processed V_2O_5 complex surface architecture. Electrochim Acta 242:382–389. https://doi.org/10.1016/j.electacta.2017.05.010
33. Mai LQ, Minhas-Khan A, Tian X, Hercule KM, Zhao YL, Lin X, Xu X (2013) Synergistic interaction between redox-active electrolyte and binder-free functionalized carbon for ultrahigh supercapacitor performance. Nat Commun 4(2923):1–7. https://doi.org/10.1038/ncomms3923
34. Sayyah SM, El-Deeb MM, Kamal SM, Azooz RE (2009) Electropolymerization of p-phenylenediamine on Pt-electrode from aqueous acidic solution: kinetic, mechanism, electrochemical studies and characterization of the polymer obtained. J Appl Polym Sci 112:3695–3706. https://doi.org/10.1002/app.31476
35. Lakouraj MM, Zare EN, Moghadam PN (2014) Synthesis of novel conductive poly(p-phenylenediamine)/Fe3O4 nanocomposite via emulsion polymerization and investigation of antioxidant activity. Adv Polym Technol 33.21385(1–7). https://doi.org/10.1002/adv.21385
36. Vinodh R, Gopi CVVM, Yang Z, Deviprasath C, Atchudan R, Raman V, Yi M, Kim H-J (2020) Novel electrode material derived from porous polymeric organic framework of phloroglucinol and terephthaldehyde for symmetric supercapacitors. J Energy Storage 28:101283. https://doi.org/10.1016/j.est.2020.101283
37. Jung HC, Vinodh R,.Gopi CVVM, Yi M, Kim H-J, Novel composite electrode material derived from hypercross-linked polymer of pyrene and polyaniline for symmetric supercapacitor. Mater Lett 257:126732. https://doi.org/10.1016/j.matlet.2019.126732
38. Atchudan R, Edison TNJI, Perumal S, Thirukumaran P, Vinodh R, Lee YR, Green synthesis of nitrogen-doped carbon nanograss for supercapacitors. J Taiwan Inst Chem E 102:475–486. https://doi.org/10.1016/j.jtice.2019.06.020